Am J Transl Res 2022;14(12):8572-8587
www.ajtr.org /ISSN:1943-8141/AJTR0138705

Original Article

Circular RNA FOXO3 regulates endometrial carcinoma progression through the microRNA-29a-3p/HDAC4 axis

Ling Yang*, Jinyin Xiao*, Chengbin Ma

*Department of Gynecology, Changning Maternity and Infant Health Hospital, East China Normal University, Shanghai 200050, China. *Equal contributors and co-first authors.*

Received August 30, 2021; Accepted April 14, 2022; Epub December 15, 2022; Published December 30, 2022

Abstract: Previous studies determined that circular RNA FOXO3 (circ_FOXO3) plays a critical role in tumorigenesis. The definite molecular mechanism of cir_FOXO3 in endometrial carcinoma (EC), nevertheless, had not been fully explored. Circ_FOXO3 expression was determined using quantitative real-time polymerase chain reaction in human EC tissues and cell lines, whereas small interfering RNAs were used to specifically silence circ_FOXO3 expression in cultured EC cells. The cell counting kit-8 assay was employed to determine the effect of ectopic circ_FOXO3 expression on cell viability. Cell proliferation and apoptosis were evaluated by flow cytometry. Further, migration and invasion of EC cells were characterized using the Transwell assay. The interaction between microRNA (miR)-29a-3p and circ_FOXO3/histone deacetylase 4 (HDAC4) was validated using dual luciferase reporter assay. Additionally, qRT-PCR and WB were employed to determine HDAC4 levels. We found that circ_FOXO3 was highly expressed in EC cells and tissues. Moreover, suppressing circ_FOXO3 expression abrogated EC by regulating cell proliferation, apoptosis, migration, and invasion. Furthermore, circ_FOXO3 could act as a sponge for miR-29a-3p, and inhibition of miR-29a-3p expression reversed the effects of circ_FOXO3 suppression on EC progression. Overexpression of miR-29a-3p inhibited EC cell growth, migration, and invasion through the regulation of HDAC4, as it is a target of miR-29a-3p. In conclusion, circ_FOXO3 promotes EC progression by sponging miR-29a-3p and upregulating HDAC4, making it a promising therapeutic target in EC.

Keywords: Circ_FOXO3, endometrial carcinoma, miR-29a-3p, HDAC4

Introduction

Endometrial carcinoma (EC) is the fourth most common malignancy worldwide, accounting for 20-30% of cancers of the female genital system [1]. It mainly affects women with an age of 55-65 years old, with a recent trend inclining toward younger ages [2]. Endometrioid carcinoma is divided into two pathologic subtypes based on its molecular and demographic features, including EC, which occurs widely and is estrogen-dependent, and non-EC, which occurs infrequently but is more aggressive and estrogen independent [3, 4]. Although advances in the understanding of neoplastic progression have markedly improved patient survival rates, the long-term prognosis of EC remains poor [5, 6]. Therefore, understanding EC's molecular mechanism and figuring out therapy targets are crucial.

Circular RNAs are a series of endogenous noncoding RNAs (ncRNAs), which are identified to be involved in the biological potential of EC [7]. One of the most important roles of circRNAs is modulating their target gene expression and influencing cancer progression by functioning as "microRNA (miRNA, miR) sponges" through direct binding [8, 9]. Circular 0000043, for instance, accelerates EC development through regulating the miR-1271-5p/CTNND1 axis [10]. Furthermore, hsa_circ_0061140 promotes EC progression by targeting the miR-149-5p/STAT axis [11]. Previous studies have confirmed the dysregulation of circ_0006404 (circ_FOXO3) expression in various cancers [12-15]. Nevertheless, the influence of circ_FOXO3 on EC has not been reported.

Histone deacetylase (HDAC) enzymes play a critical role in the regulation of histone deacetylation and promote transcriptional repression in tumorigenesis [16-18]. HDAC overexpression can promote EC progression by regulating apoptosis or the cell cycle. Thus, HDAC inhibitors have emerged as novel cancer treatment agen-

ts [19-21]. Furthermore, apicidin, a cyclic tetrapeptide extracted from *Fusarium* species, can suppress EC progression *in vivo* and *in vitro* by blocking HDAC3 and HDAC4 [22]. Thus, HDAC4 holds great potential as a therapeutic target in EC.

In the study, we first investigated the expression of circ_FOXO3 in EC-tissues as well as EC-cells and its relationship to prognosis. The influence of circular FOXO3 overexpression on multiplication, apoptosis, migration and invasion of EC cells was also investigated. Additionally, we evaluated the downstream genes and signaling pathways of circ_FOXO3 to further elucidate the mechanism through which circ_FOXO3 regulates EC development.

Materials and methods

Tissue specimens

In total, 80 pairs of EC tissues and matched para-cancerous normal tissues were obtained from patients who underwent hysterectomy. The demographic and clinical characteristics of the participants, including age, myometrial invasion, lymphatic metastasis, disease stage (International Federation of Gynecologists and Obstetricians (FIGO) 2018 criteria), and histological grade (G1, well differentiated; G2, moderately differentiated; G3, poorly differentiated) were obtained from their medical records [23]. All samples were evaluated by pathologists. Patients who accepted any treatment prior to the commencement of the research were excluded. Informed consent was obtained from each participant. The study was approved by the ethics committee of Changning Maternity and Infant Health Hospital, East China Normal University, Shanghai, P. R. China (approval number: CNFBLLKT-2020-024).

Cell culture and transfection

The EC (Ishikawa, HEC-1A, HEC-1B, HEC-251, and RL95-2) and human endometrial stromal (T-HESC) cell lines were obtained from American Type Culture Collection. RPMI 1640 medium supplemented with 10% fetal bovine serum (FBS; HyClone) as well as 100 U/mL penicillin and 100 μg/mL streptomycin was used for cell culture in a humidified 5% CO_2 incubator at 37°C. For transfection, lentivirus-mediated short hairpin RNA (shRNA) against circ_FOXO3 (sh-circ_FOXO3; 5'-ATGCATCACTCGGTTTCCTTT-3'), small interfering RNAs (siRNAs) of circ_FOXO3 (si-circ_FOXO3; 5'-AUGGAGUUCUGCUUUGCCC-3'), si-circ_FOXO3-2 (5'-GGGCAAAGCAGAACUCCAUTT-3'), miR-29a-3p mimic (5'-UAGCACCAUCUGAAAUCGGUUA-3'), miR-29a-3p inhibitor (5'-UAGCACCAUCUGAAAUCGGUUA-3'), HDAC4 overexpression vector (pc-HDAC4), and their respective controls i. e. sh-negative control [NC], (5'-CCTCTACCTGTCGCTGAGCTGTAAT-3'), si-NC (5'-GGCGGACACACAAUGUCUUTT-3'), NC mimic (5'-GCAAUCGAUGCUGAUGCGAUCGTT-3') and inhibitor (5'-CUAACGCAUGCACAGUCGUACG-3'), and pc-NC were constructed by RiboBio (Guangzhou, China) and transfected into Ishikawa cells and HEC-1B cells using Lipofectamine 3000.

Cell survival assay

CCK-8 was used to measure cell survival rate. Briefly, Ishikawa and HEC-1B cells were incubated in 96-well plates for 12 h. After induction under the indicated conditions, we added 10 μL of CCK8 reagent to the wells, then incubated for 2 h. Next, enzyme-linked immunosorbent assay was performed, and the optical density was determined at 450 nm wavelength. Each experiment was performed in triplicate.

Flow cytometry (FCM) analysis

An Annexin V-FITC Kit (JIANCHENG Biotech Co., Ltd., Shanghai, P. R. China), which uses Annexin V-FITC combined with propidium iodide (PI), was used to test apoptosis. Samples were harvested, rinsed with ice-cold PBS, and then treated with 10 μL Annexin V-FITC and 5 μL PI at ambient temperature for 15 min. The apoptosis ratio was evaluated based on Annexin V-FITC (+) cells, as apoptotic cells showed significantly higher degree of Annexin V-FITC staining, whereas dead cells demonstrated stronger staining with PI. The cells were cultured in six-well plates at the indicated conditions. The Ishikawa and HEC-1B cells were subsequently fixed using ice-cold 70% ethanol overnight. Subsequently, specimens were resuspended in PBS, cultured with RNase A, and stained with PI for 15 min. Apoptosis and cell cycle distribution were detected using FCM.

Transwell assay

The indicated cells were inoculated into the upper well of the Transwell chamber with uncoated membrane to assess their migration or

Table 1. Primers used for qRT-PCR studies

Gene	Forward Primer Sequence	Reverse Primer Sequence
circ_FOXO3	5'-CGGGATAACCAACTCTCCTTCT-3'	5'-GACGAACATTTCCTCGGCTG-3'
miR-29a-3p	5'-TTCCTCGGTAGCACCATCTG-3'	5'-TATCCTTGTTCACGACTCCTTCAC-3'
HDAC4	5'-CACGAGCACATCAAGCAACAA-3'	5'-CAGTGGTTCAGATTCCGGTGG-3'
U6	5'-AATTGGAACGATACAGAGAAG ATTAGC-3'	5'-TATGGAACGCTTCACGAAT TTG-3'
GAPDH	5'-CTGGGCTACACTGAGCACC-3'	5'-AAGTGG TCGTTGAGGGCAATG-3'

with a Matrigel-coated membrane (BD Biosciences) to determine invasion post the indicated gene transfections. The bottom chamber contained complete medium as a chemoattractant. The migrated cells were then imaged using a phase contrast light microscope and counted from five random high-power fields (hpfs) per condition.

DLR assay

The possible binding-sites of miR-29a-3p in circular FOXO3 as well as HDAC4 were forecasted using starBase. The circ_FOXO3 and HDAC4 3'-UTR sequences, with mutant (MUT) or wild-type (WT) miR-29a-3p-binding sites, were cloned into the pmirGLO luciferase reporter vector, called MUT (circ_FOXO3 MUT and HDAC4 3'-UTR MUT) or WT (circ_FOXO3 WT and HDAC4 3'-UTR WT) vectors. Ishikawa and HEC-1B-cells were co-transfected with miR-29a-3p/miR-NC as well as reporter vectors. DLR Assay System (Promega) was selected to determine activity of luciferase.

Western blotting (WB)

Proteins from EC tissues and cells were homogenized using RIPA buffer (Beyotime) and quantitated using a BCA kit (Beyotime). The samples (30 μg/lane) were resolved using SDS-PAGE at 120 V. The resolved protein bands were transferred on to a polyvinylidene fluoride membrane. Nonfat-milk (5%; Sangon Biotech, Shanghai, P. R. China) was used for blocking the membranes for 1 h under ambient temperature, which were then incubated with specific primary antibodies against HDAC4 (ab12172, 1:1,000, Abcam, Cambridge, UK) and GAPDH (ab9484, 1:5,000, Abcam, Cambridge, UK) at 4°C with gentle rocking. Subsequently, the membranes were incubated with appropriate horseradish peroxidase (HRP)-labeled secondary antibody and the signals detected using enhanced chemiluminescence (ECL) reagent (BD Biosciences) with the help of a chemiluminescence detection system.

qRT-PCR

We used TRIzol reagent to extract total RNA from EC tissues and cells. PrimeScript RT Master Mix Kit (TaKaRa, Dalian, P. R. China) and TaqMan MicroRNA RT Kit were then used to reverse transcribe RNA into cDNA. For detecting U6 and miR-29a-3p levels, Taqman Universal Master PCR Mix Kit (Thermo Fisher Scientific) was employed. The thermal program for the PCR was as follows: 95°C for 3 min and 39 cycles of 95°C for 10 s followed by 56°C for 30 s. For detecting circ_FOXO3, HDAC3, and GAPDH levels, Hieff qPCR SYBR Green Master Mix (YEASEN, Shanghai, P. R. China) was used. The thermal program for PCR was as follows: 95°C for 3 min and 39 circles of 95°C for 10 s followed by 60°C for 30 s. **Table 1** listed the primers applied in this paper. The $2^{-\Delta\Delta CT}$ method was used to analyze the relative expression of target genes.

Tumor xenotransplantation model

Female BALB/c nude mice (6-week-age) were provided by the Chinese Academy of Medical-Sciences (Beijing, China). Ishikawa cells transfected with sh-circ_FOXO3 or sh-NC were injected into the mice (six mice/group). Tumor volume was determined weekly using the following formula: volume = length × width^2/2. After 5 weeks, the mice were euthanized; tumor tissues were excised, weighed, and collected for analyzing circ_FOXO3, miR-29a-3p, and HDAC4 expression.

Statistical analysis

All data were analyzed using GraphPad Prism 7 software. The data were expressed as mean ± SD. A Student's t test or single factor analysis of variance with Dunnett's post-hoc test was

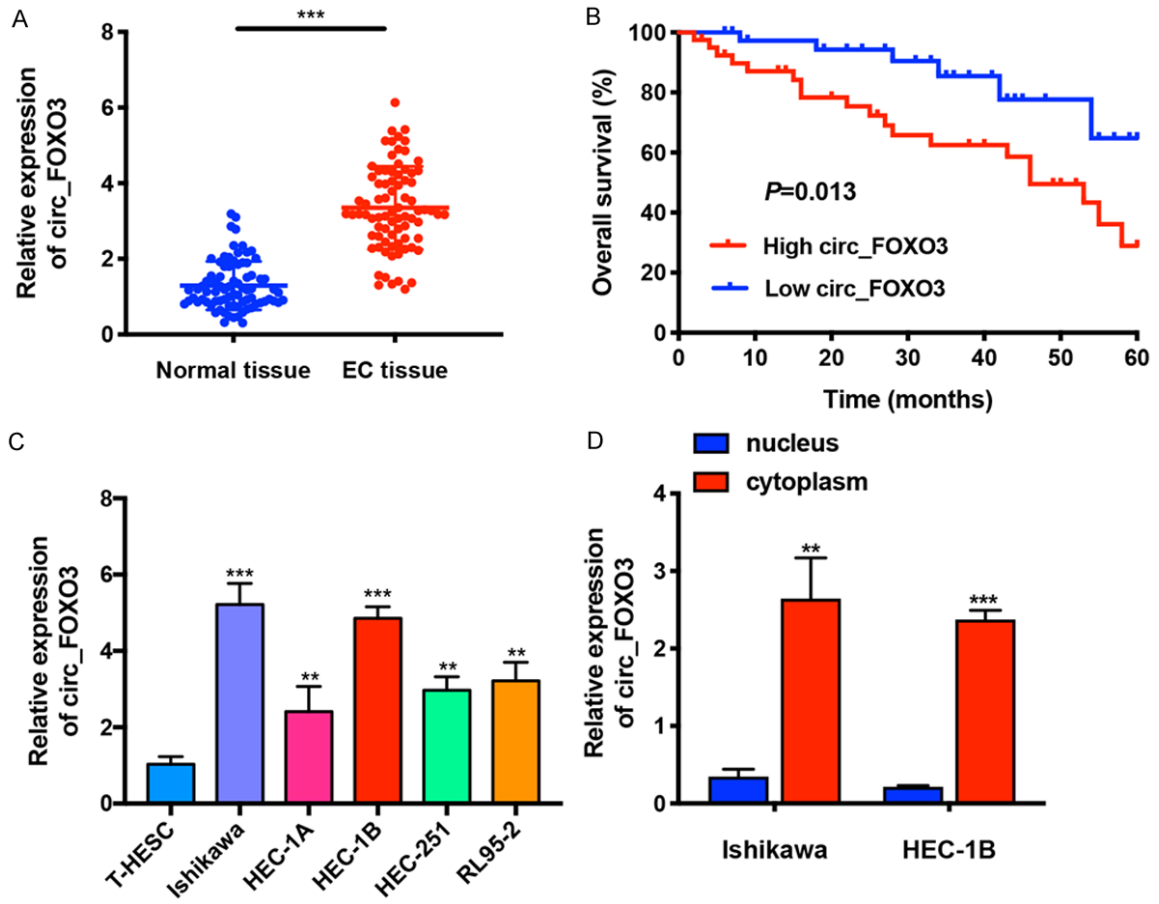

Figure 1. Circ_FOXO3 is highly expressed in EC. A. Circ_FOXO3 expression levels in 80 pairs of EC tissues and matched normal tissues were determined using qRT-PCR. B. The overall survival curve of patients with high or low circ_FOXO3 expression. C. circular FOXO3 expression level in human endometrial stromal cell-lines (T-HESC) and EC cell lines (Ishikawa, HEC-1A, HEC-1B, HEC-251, and RL95-2) detected by qRT-PCR. D. The subcellular location of circ_FOXO3 in Ishikawa and HEC-1B cells determined by qRT-PCR. *P<0.05, **P<0.01, ***P<0.001.

applied for comparison of measurement data. Pearson's Chi-square test or Fisher's exact test was conducted to test the relationship between circ_FOXO3 level and clinicopathological characteristics of EC patients. Spearman's rank coefficient of correlation was applied for evaluation of the relevance between miR-29a-3p expression and HDAC4 or circular FOXO3 expression in EC-tissues. Differences in survival rates were reviewed with Kaplan-Meier survival analysis, which were also compared with a log-rank test. P<0.05 was regarded as statistically significant.

Results

circ_FOXO3 expression is up-regulated during EC progression

The circ_FOXO3 expression was first examined in EC tissues and cell lines using qRT-PCR. circ_FOXO3 was significantly upregulated in the EC tissues as compared with that of the adjacent normal tissues (**Figure 1A**). Based on the median circ_FOXO3 expression level, we divided 80 EC patients into high and low circ_FOXO3 expression groups (n=40 each). The relationship between circ_FOXO3 expression and EC clinicopathological features and prognosis was analyzed by using survival curve analysis. Patients who had high circ_FOXO3 expression had shorter overall survival (**Figure 1B**), advanced FIGO stage (III-IV), severer histological grade, and more lymphatic metastasis (**Table 2**) than those with low circ_FOXO3 expression. Similarly, circ_FOXO3 expression was markedly increased in five representative EC cell lines, especially in the Ishikawa and HEC-1B cells, as compared with that in the stromal T-HESC cells (**Figure 1C**). Accordingly, the two cell lines with the highest circ_FOXO3 expression were selected for

Table 2. Relationship between circ_FOXO3 expression and clinicopathologic characteristics of EC patients

Data	No. of cases	circ_FOXO3		*P*-value
		low (40)	high (40)	
Age				
<50 y	35	18	17	0.822
≥50 y	45	22	23	
Myometrial invasion				
<1/2	48	26	22	0.515
≥1/2	32	13	15	
Lymphatic metastasis				
Negative	43	27	16	0.014
Positive	37	13	24	
Histologic grade				
G1	35	25	10	0.005
G2-G3	45	18	27	
FIGO stage				
I-II	40	24	16	0.025
III-IV	40	14	26	

further experiments. Moreover, we also tested the localization of circ_FOXO3 in Ishikawa and HEC-1B cells. As shown in **Figure 1D**, circ_FOXO3 was mainly located in cytoplasm. Overall, circ_FOXO3 expression was significantly upregulated in the 4 cytoplasm during the course of EC development.

Silencing circ_FOXO3 mitigates the proliferation, migration, and invasion of EC cells

To delineate the role of circ_FOXO3 in EC cells, we downregulated circ_FOXO3 in HEC-1B and Ishikawa cells using circ_FOXO3-specific siRNAs and investigated its effect on the proliferation, migration, and invasion of EC cells (si-circ_FOXO3, si-circ_FOXO3-2). qRT-PCR indicated that circ_FOXO3 expression was markedly reduced in both cell lines after transfection with si-circ_FOXO3 as compared with those transfected with si-NC and si-circ_FOXO3-2 (**Figure 2A**). Furthermore, cell apoptosis and CCK8 assays revealed that siRNA-mediated FOXO3 silencing significantly decreased the viability and increased the apoptosis of HEC-1B and Ishikawa cells (**Figure 2B** and **2C**). Flow cytometry demonstrated that circ_FOXO3 inhibition in Ishikawa and HEC-1B cells led to an elevated proportion of cells in the G0/G1 stage while reduced the number of cells in the S stage as compared with those in the control cells, suggesting that circ_FOXO3 suppression leads to blockage of EC cells at the G0/G1 stage (**Figure 2D**). Transwell migration and invasion assays further revealed that interference with circ_FOXO3 expression inhibited the migratory as well as invasive potential of Ishikawa and HEC-1B cells (**Figure 2E** and **2F**). Overall, silencing circ_FOXO3 abrogated the growth and migratory potential of EC cells.

circ_FOXO3 functions as a miR-29a-3p sponge

circRNAs can also sponge miRNAs in EC [11, 24]. To explore the mechanisms through which circ_FOXO3 affects EC development, target miRNAs of circ_FOXO3 were screened using starBase. Our studies revealed the existence of binding sites between circ_FOXO3 and miR-29a-3p (**Figure 3A**). Subsequently, DLR assays were employed to determine the relationship between circ_FOXO3 and miR-29a-3p. The luciferase activity of circ_FOXO3 WT was significantly decreased after the transfection of miR-29a-3p mimic in HEC-1B-cells as well as Ishikawa cells. The luciferase activity of circular FOXO3 MUT, nevertheless, was uninfluenced by miR-29a-3p mimic. (**Figure 3B**). Next, we tested whether circ_FOXO3 could influence miR-29a-3p expression. As anticipated, si-circ_FOXO3 indeed markedly increased miR-29a-3p expression in the Ishikawa and HEC-1B cells (**Figure 3C**). Moreover, miR-29a-3p expression was abrogated in EC tissues, showing an inverse correlation with circ_FOXO3 expression (**Figure 3D** and **3E**). Overall, miR-29a-3p is a potential target of circ_FOXO3 in EC cells.

miR-29a-3p suppression alleviates inhibitory effects of circ_FOXO3 knockdown in EC cells

To explore whether circ_FOXO3 plays a biological role by sponging miR-29a-3p, Ishikawa and HEC-1B cells were transfected with si-NC, si-circ_FOXO3, si-circ_FOXO3 + miR-29a-3p inhibitor, or si-circ_FOXO3 + miR-NC. qRT-PCR showed that circ_FOXO3 silencing elevated, whereas the miR-29a-3p inhibitor reduced, miR-29a-3p expression in Ishikawa and HEC-1B cells (**Figure 4A**). Moreover, treatment with the miR-29a-3p inhibitor alleviated the anti-proliferation as well as pro-apoptotic effects of circ_FOXO3 silencing on EC cells (**Figure 4B** and **4C**). miR-29a-3p

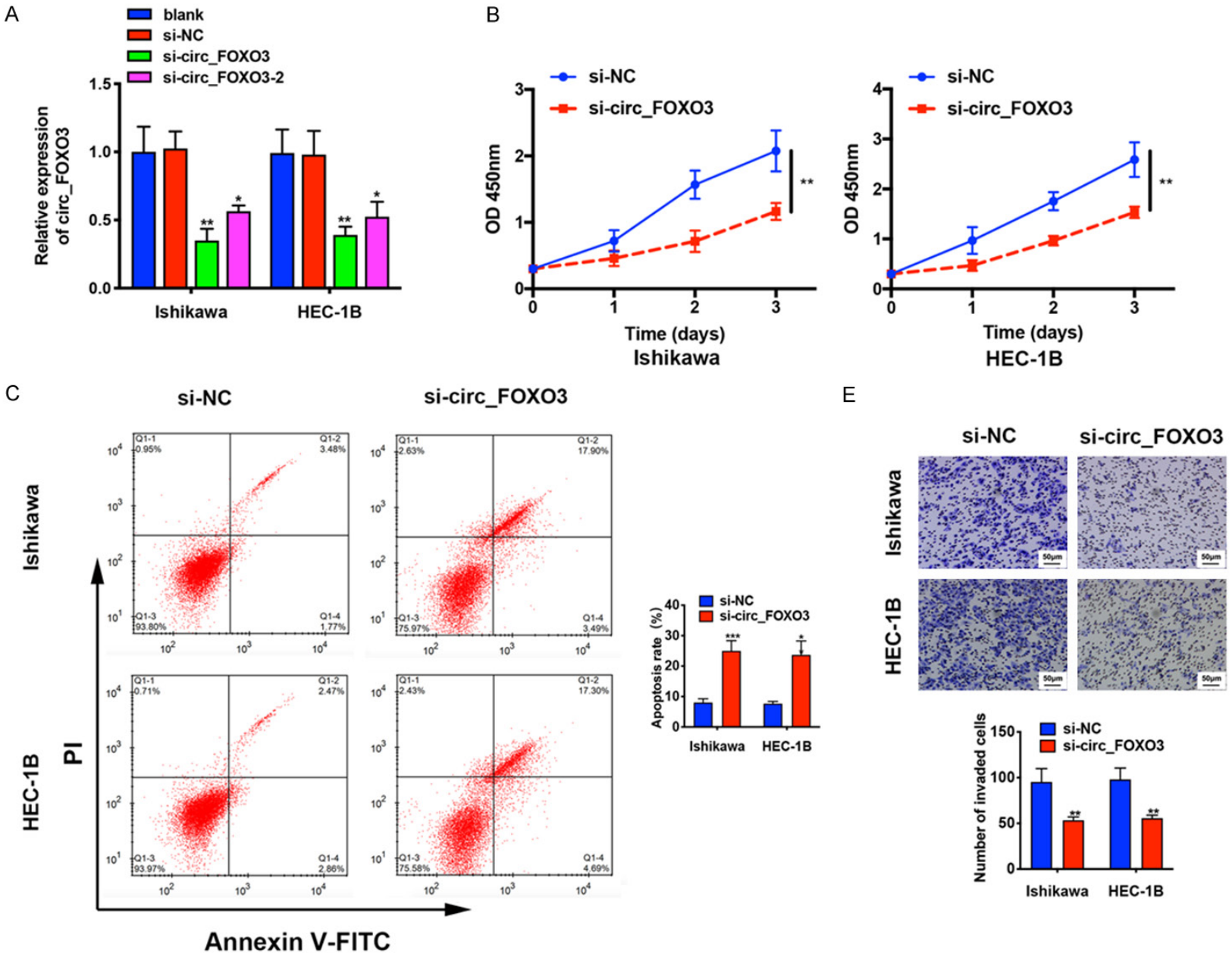
A
blank
si-NC
si-circ_FOXO3
si-circ_FOXO3-2
Relative expression of circ_FOXO3
Ishikawa
HEC-1B
B
si-NC
si-circ_FOXO3
OD 450nm
Time (days)
Ishikawa
HEC-1B
C
si-NC
si-circ_FOXO3
Ishikawa
HEC-1B
PI
Annexin V-FITC
Apoptosis rate (%)
E
si-NC
si-circ_FOXO3
Ishikawa
HEC-1B
Number of invaded cells

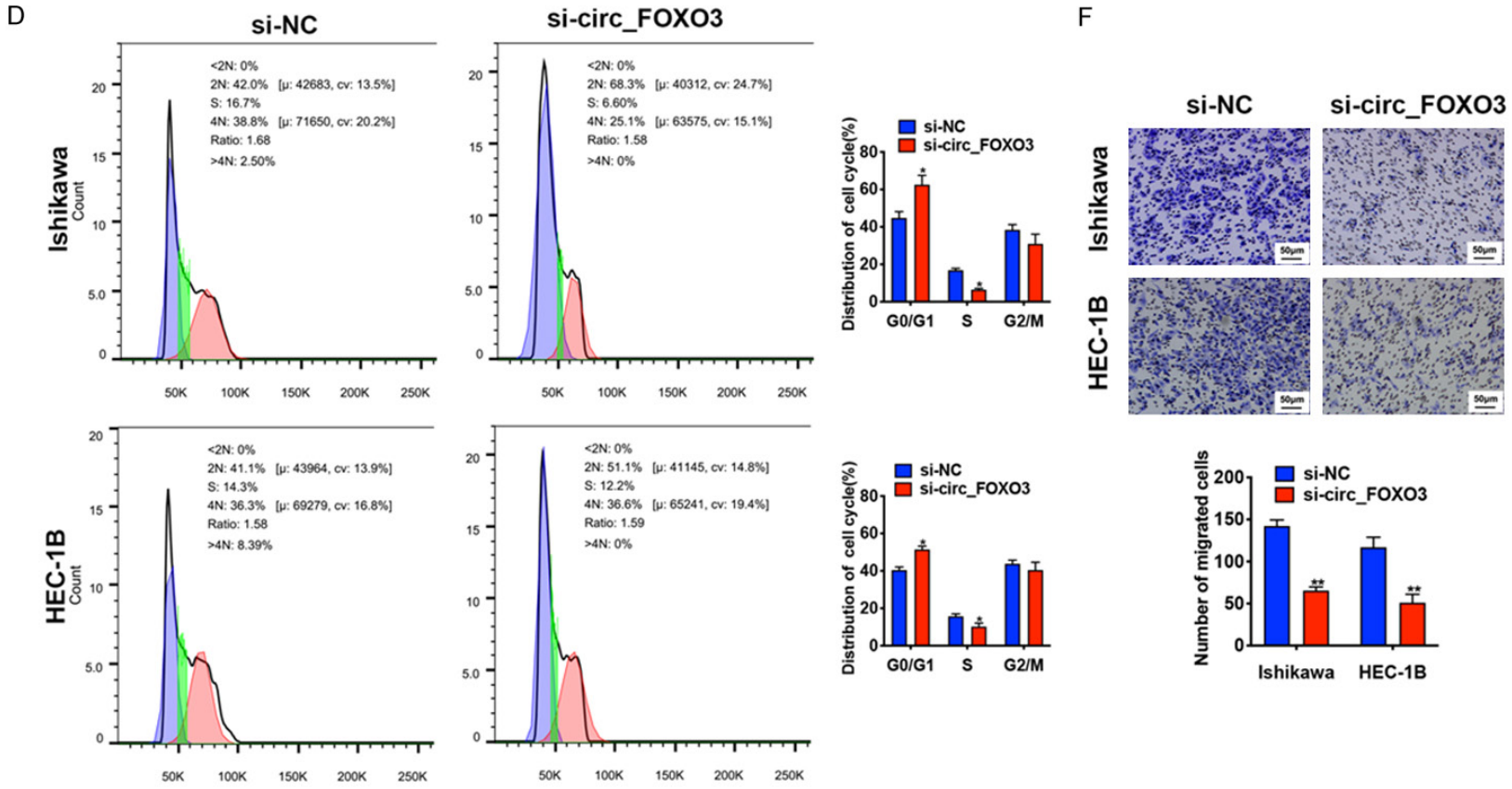

Figure 2. Circ_FOXO3 knockdown inhibits EC cell proliferation *in vitro*. (A) The knockdown effects of si-circ_FOXO3 and si-circ_FOXO3-2 were determined in Ishikawa and HEC-1B cells using qRT-PCR. (B) The CCK8 test was conducted to determine the viability of Ishikawa and HEC-1B cells after transfection with si-circ_FOXO3 or si-NC at 24, 48, and 72 h. The apoptosis (C) and cell cycle distribution (D) of HEC-1B and Ishikawa cells after transfection with si-circ_FOXO3 or si-NC were assessed using FCM. The invasion (E) and migration (F) of these cells after transfection with si-circ_FOXO3 or si-NC were assessed with Transwell assays (original magnification, ×200). *P<0.05, **P<0.01, ***P<0.001.

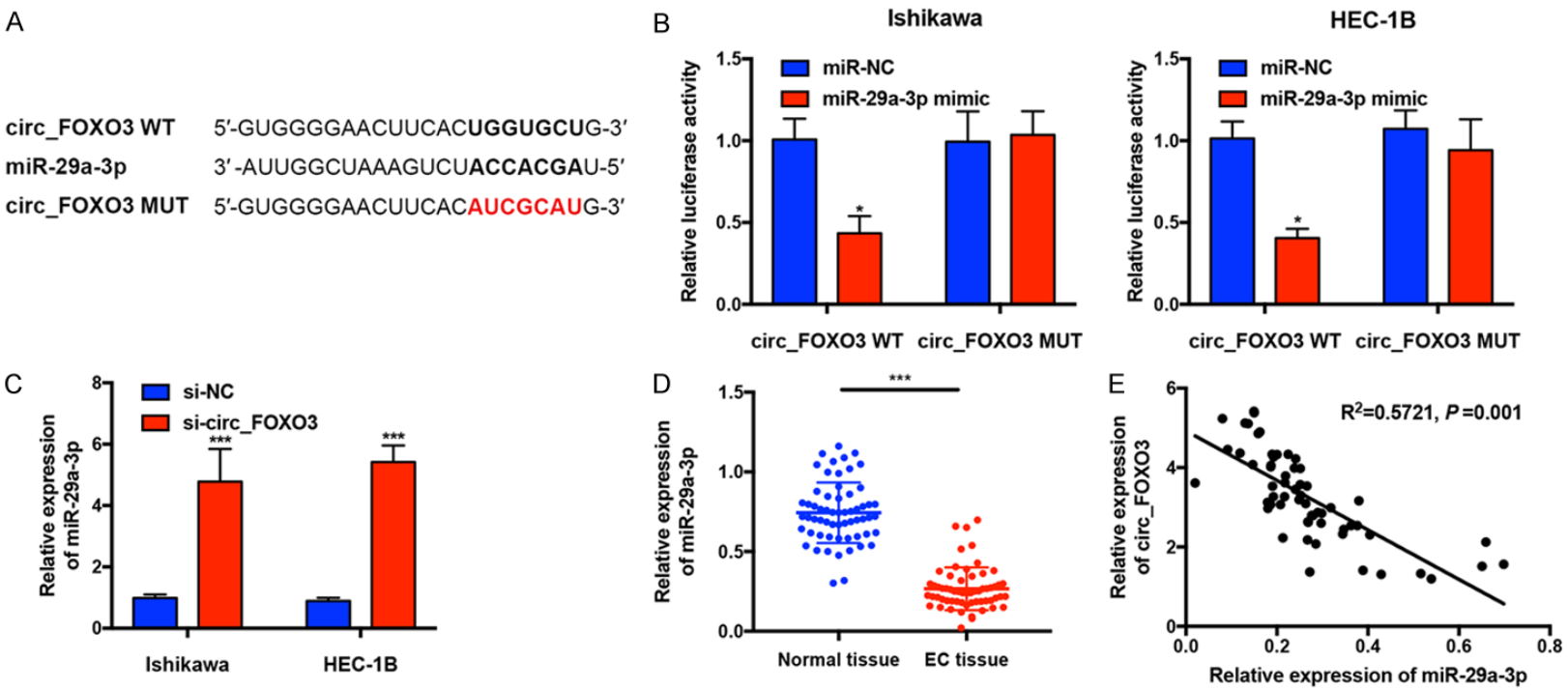

Figure 3. Circ_FOXO3 negatively regulates miR-29a-3p in EC. A. The schematic representation of binding sequence between miR-29a-3p and circ_FOXO3. B. The interaction between circ_FOXO3 and miR-29a-3p in Ishikawa and HEC-1B cells evaluated with DLR assay. C. miR-29a-3p expression after transfection with si-circ_FOXO3 or si-NC. D. Abundance of miR-29a-3p in EC tumor-tissues and adjacent normal-tissues assessed by qRT-PCR. E. Correlation analysis between circ_FOXO3 and miR-29a-3p (n=80). *P<0.05, **P<0.01, ***P<0.001.

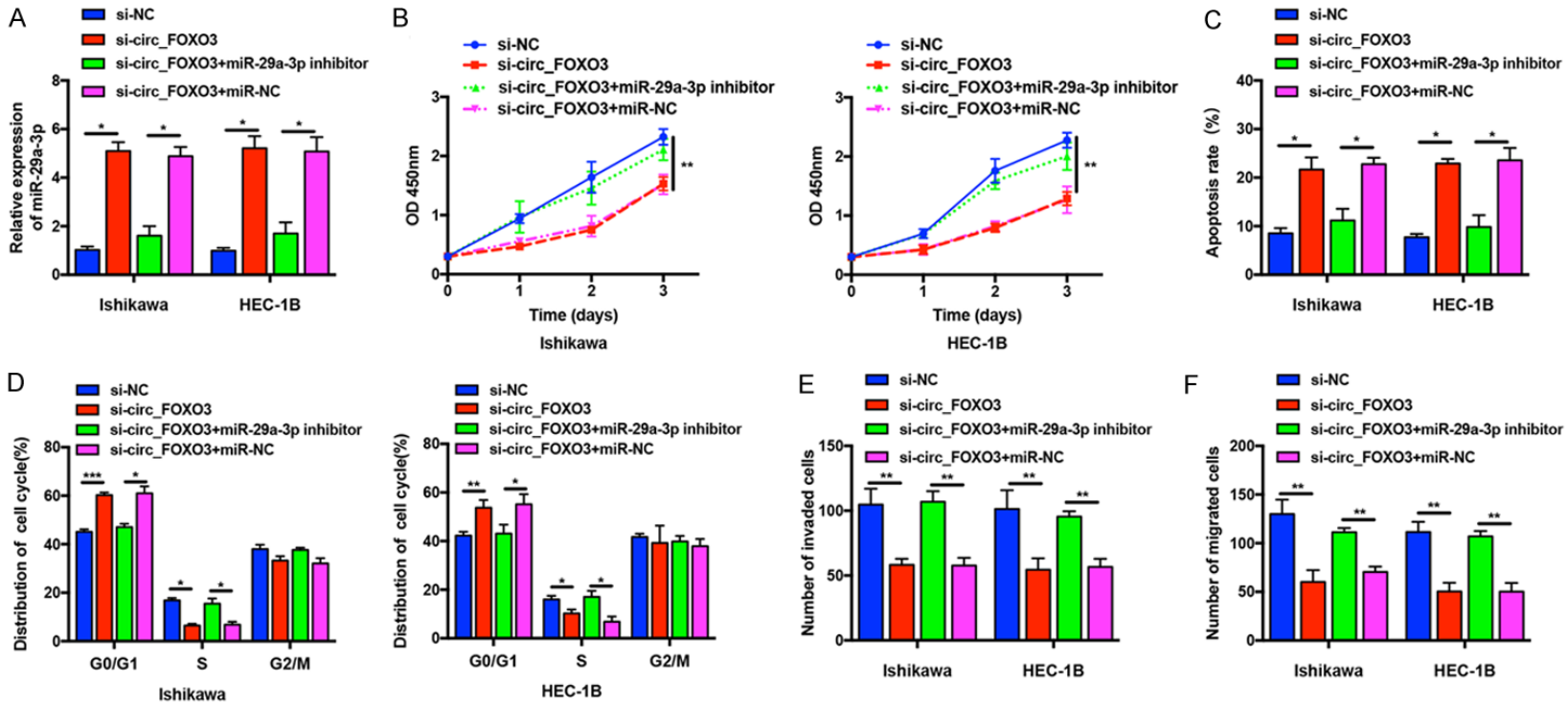

Figure 4. Downregulation of miR-29a-3p expression alleviates the inhibitory effects of circ_FOXO3 inhibition on EC progression. Ishikawa and HEC-1B cells were transfected with si-circ_FOXO3, si-NC, si-circ_FOXO3 + miR-29a-3p inhibitor, or si-circ_FOXO3 + miR-NC. A. miR-29a-3p expression in EC-cells detected with qRT-PCR. B. Viability of HEC-1B-cells and Ishikawa-cells determined through CCK8 test. C and D. Cell-apoptosis and cell cycle distribution detected by FCM. E and F. Invasion and migration of the HEC-1B and Ishikawa cells. *P<0.05, **P<0.01, ***P<0.001.

inhibition also abolished the si-circ_FOXO3-mediated cell cycle arrest (**Figure 4D**). In addition, Transwell migration as well as invasion assays demonstrated that miR-29a-3p knockdown reversed the inhibitory effects of circ_FOXO3 silencing on the migration as well as invasive properties of EC cells (**Figure 4E** and **4F**). Overall, circ_FOXO3 knockdown resulted in the inhibition of proliferation, migration, and invasion of EC cells and accelerated the apoptosis of EC cells through sponging miR-29a-3p.

HDAC4 is a direct target of miR-29a-3p

miRNAs function by interacting with the 3'-UTR of their target mRNAs. Screening for possible targets of miR-29a-3p revealed that the 3'-UTR of *HDAC4* mRNA possesses putative binding sites for miR-29a-3p (**Figure 5A**). Subsequent DLR assays showed that miR-29a-3p overexpression significantly abrogated the luciferase activity of HDAC4 3'-UTR WT, but not that of HDAC4 3'-UTR MUT, in both Ishikawa and HEC-1B cells (**Figure 5B**). Additionally, the effects of miR-29a-3p on HDAC4 expression was studied. Results of western blotting as well as qRT-PCR suggested that miR-29a-3p over-expression inhibited mRNA as well as protein expression of HDAC4 in Ishikawa and HEC-1B-cells (**Figure 5C** and **5D**). Subsequently, the expression pattern of HDAC4 in the EC tissues was studied. The results suggested the mRNA and protein levels of HDAC4 were increased in the EC-tissues in comparison to normal-tissues (**Figure 5E** and **5F**). Overall, miR-29a-3p was found to directly target HDAC4 in EC cells.

miR-29a-3p inhibits EC development by targeting HDAC4

To explore the necessity of HDAC4 for functions mediated by miR-29a-3p, we transfected Ishikawa and HEC-1B-cells with pc-HDAC4, miR-29a-3p mimic, miR-29a-3p mimic & miR-NC, or miR-29a-3p mimic & pc-NC. Subsequent assessment of these cells revealed that miR-29a-3p-mediated reduction in HDAC4 expression was reversed upon transfection of EC cells with pc-HDAC4 (**Figure 6A**). Moreover, miR-29a-3p overexpression led to inhibition of cell viability, which was subsequently mitigated upon HDAC4 overexpression (**Figure 6B**). Additionally, miR-29a-3p mimic facilitated apoptosis as well as G0/G1 cell-cycle arrest and these effects were weakened by HDAC4 upregulation (**Figure 6C** and **6D**). Furthermore, the reduced migration and invasion brought by miR-29a-3p overexpression was abolished by transfection with pc-HDAC4 (**Figure 6E** and **6F**). Overall, miR-29a-3p inhibited EC cell progression by downregulating HDAC4.

circ_FOXO3 silencing hinders EC development through the miR-29a-3p/HDAC4 axis in vivo

The sh_circ_FOXO3 group showed decreased tumor volume and weight compared to the sh-NC group (**Figure 7A-C**). qRT-PCR showed that circ_FOXO3 expression was significantly decreased in the tumors from the sh-circ_FOXO3 group compared to the sh-NC group (**Figure 7D**). Moreover, miR-29a-3p expression was increased, whereas that of HDAC4 was abrogated, in the tumors from the sh_circ_FOXO3 group compared to the sh-NC group (**Figure 7E-G**). Altogether, these results suggest that suppression of circ_FOXO3 expression abrogates EC progression through the miR-29a-3p/HDAC4 axis.

Discussion

circRNAs are abnormally expressed in multiple pathophysiological conditions, including cancer. In this study, we observed that circular FOXO3 had been up-regulated in the EC-tissues and that inhibition of circ_FOXO3 suppresses EC cell-multiplication, migration, and invasion, indicating an oncogenic role of circ_FOXO3. Moreover, circ_FOXO3 suppression resulted in downregulation of HDAC4 by increasing the expression of miR-29a-3p, suggesting a significant role of the circ_FOXO3/miR-29a-3p/HDAC4 axis in EC development.

The role of circ_FOXO3 in tumor development has been explored in various cancers. circ_FOXO3 expression has been determined to be highly elevated in glioblastomas compared to low-grade gliomas. circ_FOXO3 knockdown has been shown to inhibit glioblastoma tumorigenesis and invasion, while its overexpression aggravates these effects [25]. Furthermore, circ_FOXO3 is upregulated in gastric carcinoma, whereas its overexpression promotes neoplastic growth *in vitro* and *in vivo* [15]. Additionally, strong circ_FOXO3 expression has been shown to induce adriamycin resistance in hepatocellular carcinoma by decreasing miR-199a-5p expression [26]. However, previous

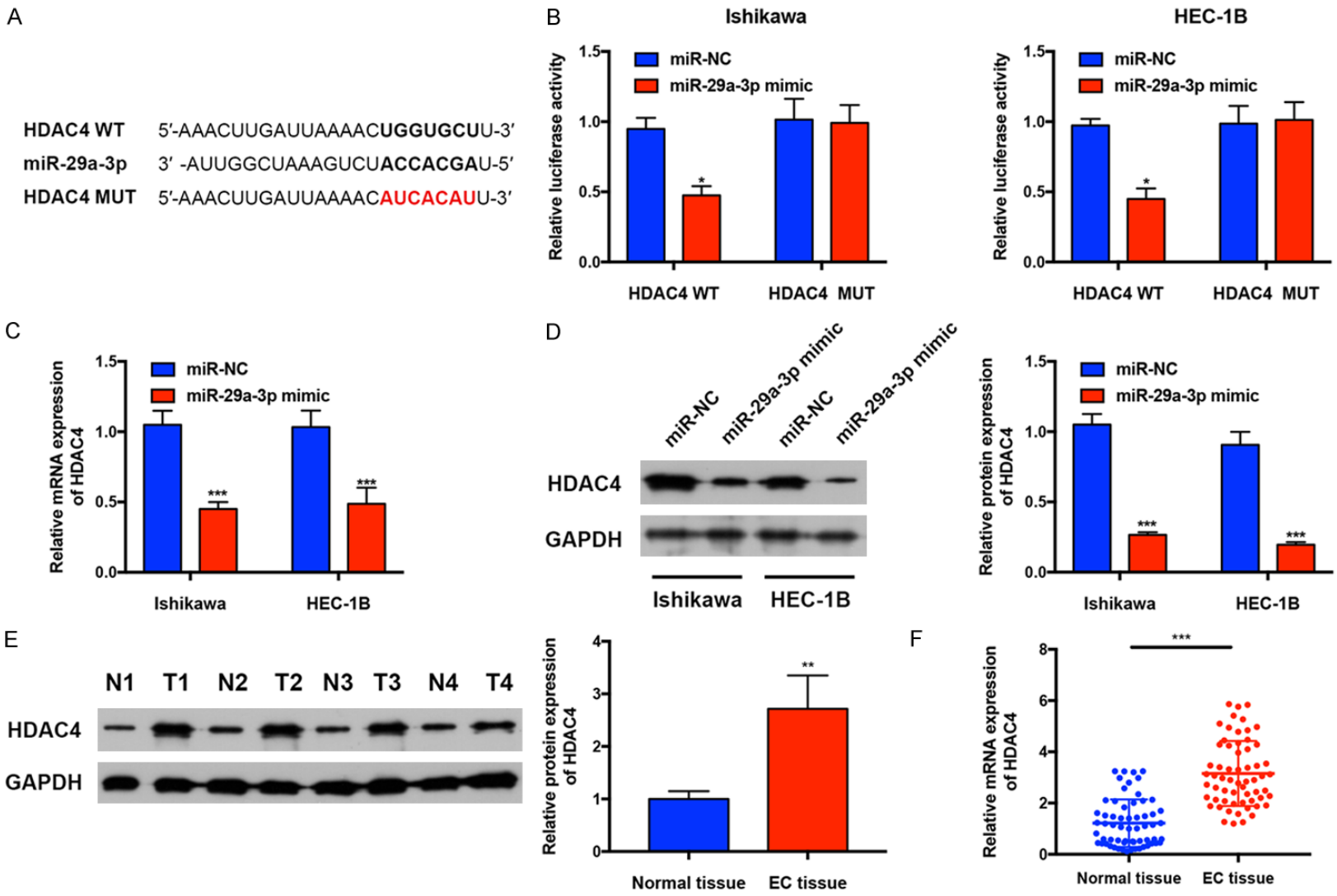

Figure 5. HDAC4 is a functional target of miR-29a-3p. A. The binding sites between miR-29a-3p and HDAC4 were predicted by TargetScan. B. Luciferase activity was measured in Ishikawa as well as HEC-1B cells, which were co-transfected with miR-NC or miR-29a-3p mimic and HDAC4 3'-UTR-WT or HDAC4 3'-UTR-MUT. C, D. HDAC4 expression at the mRNA and protein levels was examined in Ishikawa and HEC-1B cells, post co-transfection with miR-NC or miR-29a-3p mimic, using qRT-PCR and WB respectively. E, F. HDAC4 expression at the protein and mRNA levels was identified in EC and adjacent normal tissues through WB and qRT-PCR respectively. *P<0.05, **P<0.01, ***P<0.001.

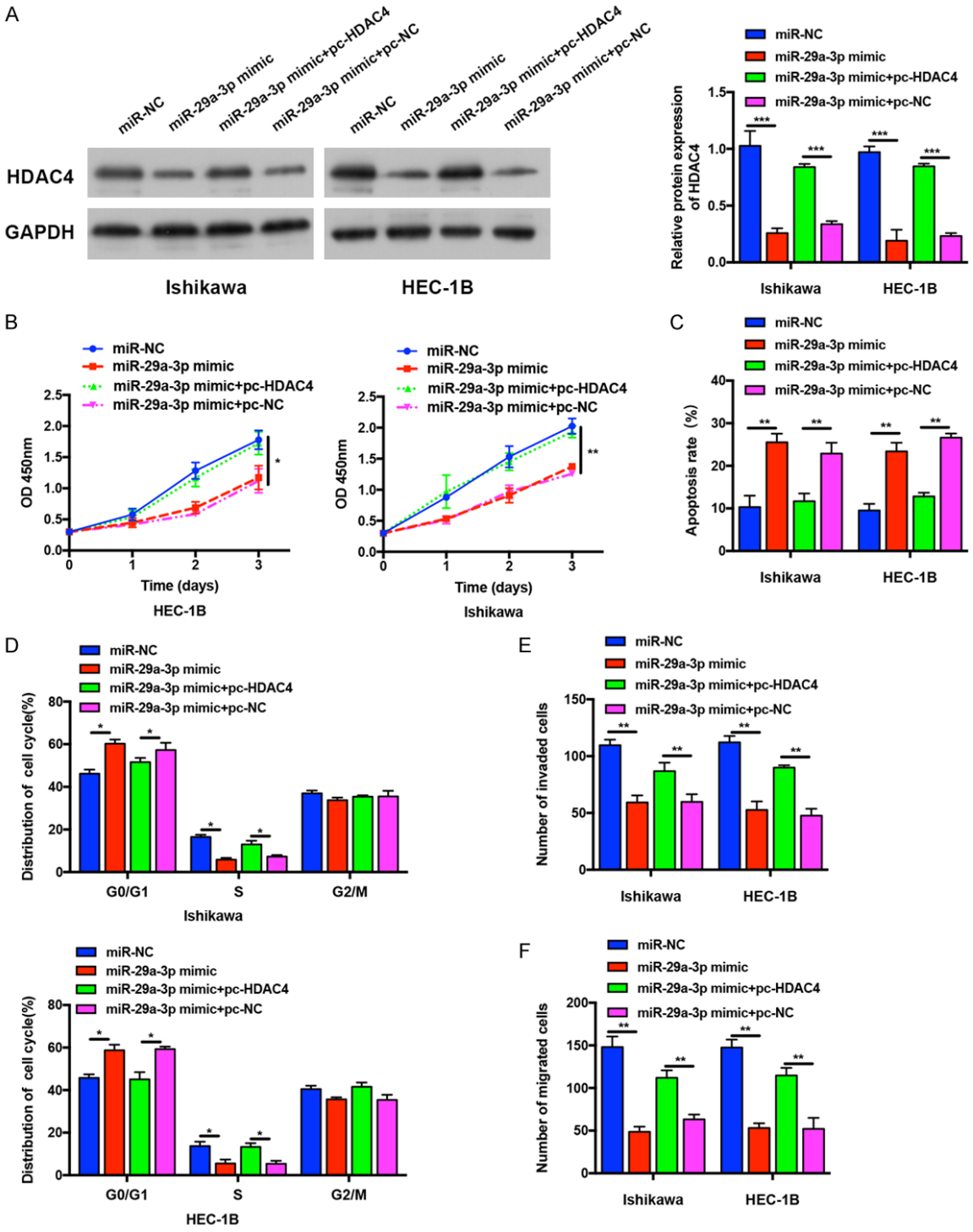

Figure 6. Overexpression of miR-29a-3p inhibits EC cell growth, migration, and invasion through the regulation of HDAC4. (A) HDAC4 protein abundance was detected in Ishikawa and HEC-1B cells post miR-NC, miR-29a-3p mimic + pc-HDAC4, miR-29a-3p mimic, or miR-29a-3p mimic + pc-NC transfection. (B) Viability of HEC-1B and Ishikawa cells after transfection was measured using the CCK8 assay. Apoptosis (C) and cell cycle distribution (D) of Ishikawa and HEC-1B cells after transfection by using FCM. (E and F) Invasion and migration assays of HEC-1B and Ishikawa cells after transfection. *P<0.05, **P<0.01, ***P<0.001.

studies have also identified that circ_FOXO3 levels are decreased in urothelial carcinoma, non-small-cell lung carcinoma, and urinary bladder carcinoma [13, 14, 27]. To the best of

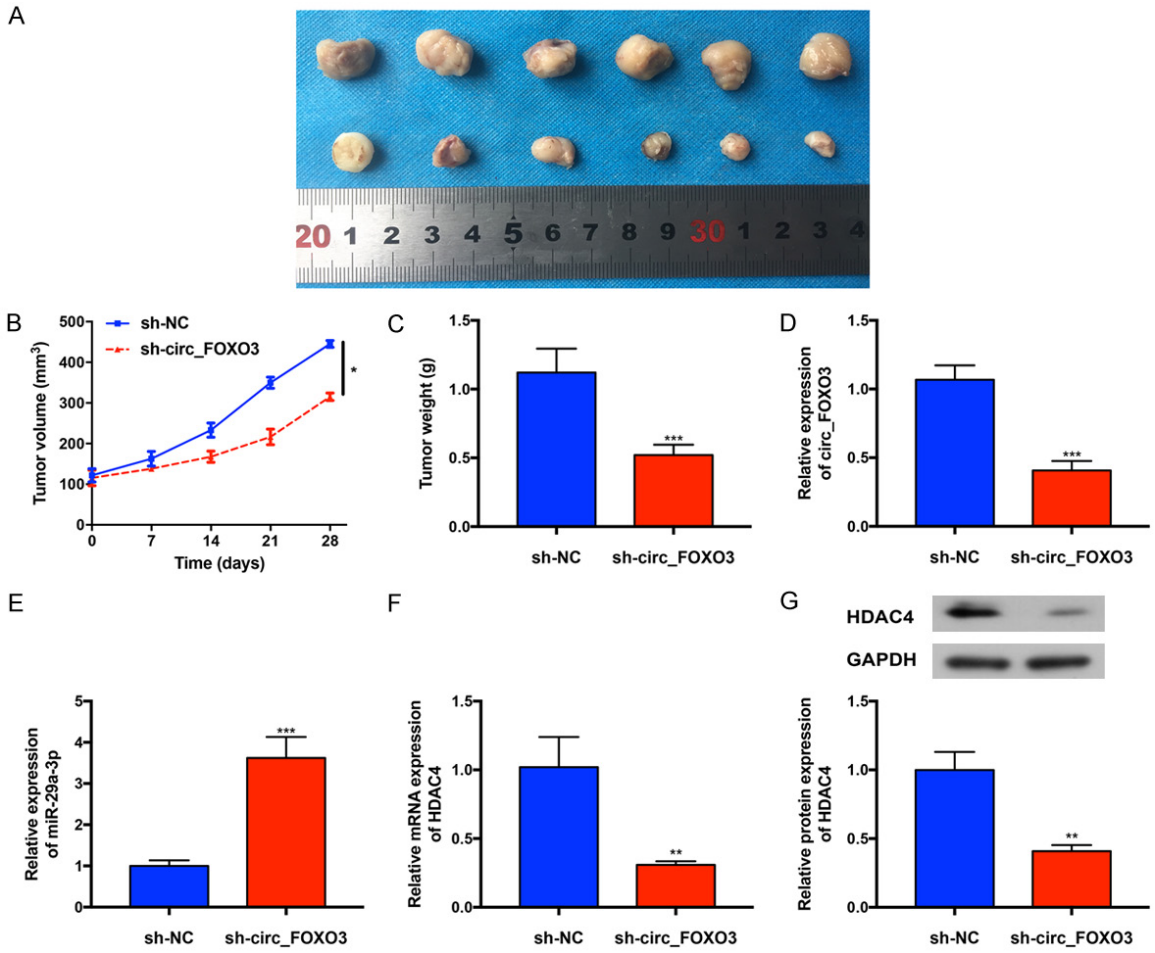

Figure 7. Knockdown of circ_FOXO3 inhibits EC tumor growth *in vivo*. (A) Tumor formation in xenografts of nude mice (n=6). Average tumor volumes (B) and tumor weights (C) of each group (n=6/group). Measured circ_FOXO3 (D), miR-29a-3p (E), and HDAC4 (F) levels in tumor tissues by using qRT-PCR. (G) Western blotting results of HDAC4 protein expression after transfection with sh-circ_FOXO3 or sh-NC. *P<0.05, **P<0.01, ***P<0.001.

our knowledge, no study has explored the role of circ_FOXO3 in EC so far. In the current study, circ_FOXO3 showed high expression in EC tissues and contributed to the poor survival of EC patients. Furthermore, inhibition of circ_FOXO3 expression was also determined to decrease EC progression both *in vitro* and *in vivo*. Overall, circ_FOXO3 exerts a significant effect on EC progression.

circRNAs interact with miRNAs and function as competing endogenous RNAs (ceRNAs), resulting in the suppression of downstream target mRNAs, and participate in the process of tumorigenesis [8, 28]. Notably, circ_FOXO3 is a documented miRNA sponge that regulates various miRNAs, including miR-191-5p, miR-155, miR-605, and miR-9-5p [13, 14, 27, 29]. Furthermore, previous studies also proved that the expression of miR-191-5p, miR-155, and miR-9-5p was increased in EC tissues, which might be associated with the development of EC [30-33]. Exploring the relationship between circ_FOXO3 and miRNAs in EC might find new therapeutic targets in the future. Herein, miR-29a-3p was confirmed as a valid target of circ_FOXO3. Ma et al. reported that miR-29a-3p contributes to suppression of tumor progression. For instance, miR-29a-3p repressed the cell growth as well as invasion of papillary carcinoma of the thyroid through controlling the OTUB2 signaling pathway [34]. Chen et al. showed that cervical carcinoma cell proliferation and migration are suppressed by miR-29a-3p that regulates the *SNIP1* gene [35]. Similarly, we observed decreased miR-29a-3p expression in EC in the present study. Our findings revealed that miR-29a-3p overexpression reverses the inhibitory

effects of si-circ_FOXO3 on viability, apoptosis, cell cycle, migration, and invasion in EC cells. Furthermore, we have illustrated an inverse correlation between circ_FOXO3 and miR-29a-3p in EC tissues. Overall, our results provide strong evidence supporting critical role of circ_FOXO3 by sponging miR-29a-3p in EC progression.

Our bioinformatic studies through TargetScan and DLR assays have shown that HDAC4 is directly bound to miR-29a-3p. HDAC4 is a lysine deacetylase that deacetylates histone and non-histone proteins, which are critical in regulating cell proliferation and apoptosis, DNA damage, and other cellular processes in cancer [36, 37]. Wang et al. have revealed that deacetylation of SP1 and KLF5 mediated by HDAC4 promotes the activity of the JNK/c-Jun pathway, thereby facilitating glioma formation [38]. Moreover, HDAC4 is overexpressed in EC, and HDAC inhibitors have been shown to inhibit EC cell growth [39, 40]. Consistently, upregulated HDAC4 expression has been observed in EC tissues, and HDAC4 overexpression has been shown to attenuate the antitumor effect of the miR-29a-3p mimics in EC cells. In addition, our *in vivo* experiments have also confirmed that circ_FOXO3 upregulates the expression of HDAC4 in EC tumor tissues by decreasing miR-29a-3p levels. Thus, our overall data indicate that the circ_FOXO3/miR-29a-3p/HDAC4 axis contributes significantly to the development of EC.

There were certain limitations to our study. As per our *in silico* studies, miR-29a-3p is not the only target for circ_FOXO3. There may be indeed multiple mechanisms by which circ_FOXO3 participate in regulating EC development. Therefore, detailed investigations should be performed to explore the role of circ_FOXO3 in EC progression. In the present study, only knockdown studies for circ_FOXO3 were performed. For detailed delineation of the role of circ_FOXO3 in EC progression, the effects of overexpression of circ_FOXO3 should also be investigated.

Conclusions

Results confirmed the upregulation of circ_FOXO3 and HDAC4, and the downregulation of miR-29a-3p in EC. Circ_FOXO3 has been shown to promote cell multiplication, migration as well as invasion through the miR-29a-3p/HDAC4 axis in EC, which might be a promising target for treating these subjects.

Acknowledgements

This work was supported by the Research Project of Changning District Science and Technology Committee (grant number CNKW2020-Y29).

Disclosure of conflict of interest

None.

Address correspondence to: Chengbin Ma, Department of Gynecology, Changning Maternity and Infant Health Hospital, East China Normal University, No. 786, Yuyuan Road, Changning District, Shanghai 200050, China. Tel: +86-13661900280; E-mail: cbma1966@sina.com

References

[1] Siegel RL, Miller KD and Jemal A. Cancer statistics, 2018. CA Cancer J Clin 2018; 68: 7-30.

[2] Lu KH and Broaddus RR. Endometrial cancer. N Engl J Med 2020; 383: 2053-2064.

[3] Goebel EA, Vidal A, Matias-Guiu X and Blake Gilks C. The evolution of endometrial carcinoma classification through application of immunohistochemistry and molecular diagnostics: past, present and future. Virchows Arch 2018; 472: 885-896.

[4] Bell DW and Ellenson LH. Molecular genetics of endometrial carcinoma. Annu Rev Pathol 2019; 14: 339-367.

[5] Reijnen C, Gogou E, Visser NCM, Engerud H, Ramjith J, van der Putten LJM, van de Vijver K, Santacana M, Bronsert P, Bulten J, Hirschfeld M, Colas E, Gil-Moreno A, Reques A, Mancebo G, Krakstad C, Trovik J, Haldorsen IS, Huvila J, Koskas M, Weinberger V, Bednarikova M, Hausnerova J, van der Wurff AAM, Matias-Guiu X, Amant F, Massuger LFAG, Snijders MPLM, Küsters-Vandevelde HVN, Lucas PJF and Pijnenborg JMA; ENITEC Consortium. Pre-operative risk stratification in endometrial cancer (ENDORISK) by a Bayesian network model: a development and validation study. PLoS Med 2020; 17: e1003111.

[6] Bradford LS, Rauh-Hain JA, Schorge J, Birrer MJ and Dizon DS. Advances in the management of recurrent endometrial cancer. Am J Clin Oncol 2015; 38: 206-212.

[7] Razavi ZS, Tajiknia V, Majidi S, Ghandali M, Mirzaei HR, Rahimian N, Hamblin MR and Mirzaei H. Gynecologic cancers and non-cod-

ing RNAs: epigenetic regulators with emerging roles. Crit Rev Oncol Hematol 2021; 157: 103192.
[8] Bach DH, Lee SK and Sood AK. Circular RNAs in cancer. Mol Ther Nucleic Acids 2019; 16: 118-129.
[9] Zhang Z, Yang T and Xiao J. Circular RNAs: promising biomarkers for human diseases. EBioMedicine 2018; 34: 267-274.
[10] Wei D, Tian M, Fan W, Zhong X, Wang S, Chen Y and Zhang S. Circular RNA circ_0000043 promotes endometrial carcinoma progression by regulating miR-1271-5p/CTNND1 axis. Arch Gynecol Obstet 2021; 303: 1075-1087.
[11] Liu Y, Chang Y and Cai Y. Hsa_circ_0061140 promotes endometrial carcinoma progression via regulating miR-149-5p/STAT3. Gene 2020; 745: 144625.
[12] Shen Z, Zhou L, Zhang C and Xu J. Reduction of circular RNA Foxo3 promotes prostate cancer progression and chemoresistance to docetaxel. Cancer Lett 2020; 468: 88-101.
[13] Wang C, Tao W, Ni S and Chen Q. Circular RNA circ-Foxo3 induced cell apoptosis in urothelial carcinoma via interaction with miR-191-5p. Onco Targets Ther 2019; 12: 8085-8094.
[14] Li Y, Qiao L, Zang Y, Ni W and Xu Z. Circular RNA FOXO3 suppresses bladder cancer progression and metastasis by regulating MiR-9-5p/TGFBR2. Cancer Manag Res 2020; 12: 5049-5056.
[15] Xiang T, Jiang HS, Zhang BT and Liu G. CircFOXO3 functions as a molecular sponge for miR-143-3p to promote the progression of gastric carcinoma via upregulating USP44. Gene 2020; 753: 144798.
[16] Liu T, Wan Y, Xiao Y, Xia C and Duan G. Dual-Target inhibitors based on HDACs: novel antitumor agents for cancer therapy. J Med Chem 2020; 63: 8977-9002.
[17] Li Y and Seto E. HDACs and HDAC inhibitors in cancer development and therapy. Cold Spring Harb Perspect Med 2016; 6: a026831.
[18] Manzotti G, Torricelli F, Donati B, Sancisi V, Gugnoni M and Ciarrocchi A. HDACs control RUNX2 expression in cancer cells through redundant and cell context-dependent mechanisms. J Exp Clin Cancer Res 2019; 38: 346.
[19] Yoshioka T, Yogosawa S, Yamada T, Kitawaki J and Sakai T. Combination of a novel HDAC inhibitor OBP-801/YM753 and a PI3K inhibitor LY294002 synergistically induces apoptosis in human endometrial carcinoma cells due to increase of Bim with accumulation of ROS. Gynecol Oncol 2013; 129: 425-32.
[20] Yi TZ, Li J, Han X, Guo J, Qu Q, Guo L, Sun HD and Tan WH. DNMT inhibitors and HDAC inhibitors regulate E-cadherin and Bcl-2 expression in endometrial carcinoma in vitro and in vivo. Chemotherapy 2012; 58: 19-29.
[21] Li LH, Zhang PR, Cai PY and Li ZC. Histone deacetylase inhibitor, Romidepsin (FK228) inhibits endometrial cancer cell growth through augmentation of p53-p21 pathway. Biomed Pharmacother 2016: 82: 161-6.
[22] Ahn MY, Chung HY, Choi WS, Lee BM, Yoon S and Kim HS. Anti-tumor effect of apicidin on Ishikawa human endometrial cancer cells both in vitro and in vivo by blocking histone deacetylase 3 and 4. Int J Oncol 2010; 36: 125-31.
[23] Grigsby PW, Massad LS, Mutch DG, Powell MA, Thaker PH, McCourt C, Hagemann A, Fuh K, Kuroki L and Schwarz JK. FIGO 2018 staging criteria for cervical cancer: impact on stage migration and survival. Gynecol Oncol 2020; 157: 639-643.
[24] Shen Q, He T and Yuan H. Hsa_circ_0002577 promotes endometrial carcinoma progression via regulating miR-197/CTNND1 axis and activating Wnt/beta-catenin pathway. Cell Cycle 2019; 18: 1229-1240.
[25] Zhang S, Liao K, Miao Z, Wang Q, Miao Y, Guo Z, Qiu Y, Chen B, Ren L, Wei Z, Lin Y, Lu X and Qiu Y. CircFOXO3 promotes glioblastoma progression by acting as a competing endogenous RNA for NFAT5. Neuro Oncol 2019; 21: 1284-1296.
[26] Huang W, Huang F and Feng C. CircFoxo3 promotes adriamycin resistance through regulation of miR-199a-5p/ATP binding cassette subfamily C member 1 axis in hepatocellular carcinoma. Onco Targets Ther 2020; 13: 5113-5122.
[27] Zhang Y, Zhao H and Zhang L. Identification of the tumorsuppressive function of circular RNA FOXO3 in nonsmall cell lung cancer through sponging miR155. Mol Med Rep 2018; 17: 7692-7700.
[28] Yang C, Wu S, Wu X, Zhou X, Jin S and Jiang H. Silencing circular RNA UVRAG inhibits bladder cancer growth and metastasis by targeting the microRNA-223/fibroblast growth factor receptor 2 axis. Cancer Sci 2019; 110: 99-106.
[29] Li J, Qin X, Wu R, Wan L, Zhang L and Liu R. Circular RNA circFBXO11 modulates hepatocellular carcinoma progress and oxaliplatin resistance through miR-605/FOXO3/ABCB1 axis. J Cell Mol Med 2020; 24: 5152-5161.
[30] Myatt SS, Wang J, Monteiro LJ, Christian M, Ho KK, Fusi L, Dina RE, Brosens JJ, Ghaem-Maghami S and Lam EW. Definition of microRNAs that repress expression of the tumor suppressor gene FOXO1 in endometrial cancer. Cancer Res 2010; 70: 367-377.
[31] Choi CH, Park YA, Choi JJ, Song T, Song SY, Lee YY, Lee JW, Kim TJ, Kim BG and Bae DS. Angiotensin II type I receptor and miR-155 in endometrial cancers: synergistic antiproliferative effects of anti-miR-155 and losartan on

endometrial cancer cells. Gynecol Oncol 2012; 126: 124-131.
[32] Torres A, Torres K, Pesci A, Ceccaroni M, Paszkowski T, Cassandrini P, Zamboni G and Maciejewski R. Diagnostic and prognostic significance of miRNA signatures in tissues and plasma of endometrioid endometrial carcinoma patients. Int J Cancer 2013; 132: 1633-1645.
[33] Yang C, Ota-Kurogi N, Ikeda K, Okumura T, Horie-Inoue K, Takeda S and Inoue S. MicroRNA-191 regulates endometrial cancer cell growth via TET1-mediated epigenetic modulation of APC. J Biochem 2020; 168: 7-14.
[34] Ma Y and Sun Y. miR-29a-3p inhibits growth, proliferation, and invasion of papillary thyroid carcinoma by suppressing NF kappa B signaling via direct targeting of OTUB2. Cancer Manag Res 2018; 11: 13-23.
[35] Chen Y, Zhang W, Yan L, Zheng P and Li J. miR-29a-3p directly targets Smad nuclear interacting protein 1 and inhibits the migration and proliferation of cervical cancer HeLa cells. PeerJ 2020; 8: e10148.
[36] Li Y and Seto E. HDACs and HDAC inhibitors in cancer development and therapy. Cold Spring Harb Perspect Med 2016; 6: a026831.
[37] Liu T, Wan Y, Xiao Y, Xia C and Duan G. Dual-target inhibitors based on HDACs: novel antitumor agents for cancer therapy. J Med Chem 2020; 63: 8977-9002.
[38] Wang Y, Xia Y, Hu K, Zeng M, Zhi C, Lai M, Wu L, Liu S, Zeng S, Huang Z, Ma S and Yuan Z. MKK7 transcription positively or negatively regulated by SP1 and KLF5 depends on HDAC4 activity in glioma. Int J Cancer 2019; 145: 2496-2508.
[39] Li LH, Zhang PR, Cai PY and Li ZC. Histone deacetylase inhibitor, Romidepsin (FK228) inhibits endometrial cancer cell growth through augmentation of p53-p21 pathway. Biomed Pharmacother 2016; 82: 161-166.
[40] Ahn MY, Chung HY, Choi WS, Lee BM, Yoon S and Kim HS. Anti-tumor effect of apicidin on Ishikawa human endometrial cancer cells both in vitro and in vivo by blocking histone deacetylase 3 and 4. Int J Oncol 2010; 36: 125-31.